Variation of the Network Anisotropy of Cholesteric Side Chain Elastomers

ARTICLE *in* MACROMOLECULES · OCTOBER 2006

Impact Factor: 5.8 · DOI: 10.1021/ma061065a

6 AUTHORS, INCLUDING:

Juergen Schmidtke
Universität Paderborn
21 PUBLICATIONS **800** CITATIONS

Variation of the Network Anisotropy of Cholesteric Side Chain Elastomers

Christian Bourgerette,[†] Bin Chen,[‡] Heino Finkelmann,*[,‡] Michel Mitov,[†] Jürgen Schmidtke,[§] and Werner Stille*[,§]

Centre d'Elaboration de Matériaux et d'Etudes Structurales, CNRS, BP 94347, 31055 Toulouse Cedex 4, France; Institut für Makromolekulare Chemie, Albert-Ludwigs-Universität, Stefan-Meier-Str. 31, 79104 Freiburg, Germany; and Physikalisches Institut, Albert-Ludwigs-Universität, Hermann-Herder-Str. 3, 79104 Freiburg, Germany

Received May 11, 2006; Revised Manuscript Received August 31, 2006

ABSTRACT: A series of cholesteric side chain elastomers with odd and even numbers of atoms along the spacer chain were prepared. Varying the content of odd and even spacer groups resulted in anisotropic main chain conformations changing from prolate to oblate. The conformation anisotropy was characterized by temperature-dependent measurements of the sample dimensions. The transmission spectra for polarized light of the elastomer films were recorded under uniaxial mechanical stress, applied perpendicular to the helical axis of the cholesteric liquid crystal. With increasing strain a blue shift of the selective reflection due to a contraction of the helix along its axis was observed. In the case of a nonvanishing conformation anisotropy in addition a distortion of the regular helical structure was indicated by changes in the transmission spectra for linearly polarized light. This distortion was found to be much weaker than predicted by theory.

Introduction

Liquid crystalline elastomers[1] combine the rubber elasticity of lightly cross-linked polymer chains with the orientational order of liquid crystals. In nematic side chain polymers and elastomers mesogenic side groups are attached to a polymer backbone by flexible spacers. In general, the interaction of the orientationally ordered nematic side groups with the main chain segments causes anisotropic main chain conformations, as can be shown by neutron scattering experiments.[2,3] When the main segments preferentially orient parallel to the nematic director, the conformation is referred to as prolate; when they preferentially orient perpendicular, the conformation is referred to as oblate. The anisotropic conformation is the origin of a coupling between the nematic order and the network; i.e., the director field can be affected by mechanical stress. When the side groups (at least partially) are chiral, a helically twisted nematic director field (the so-called cholesteric structure) is obtained. One of the unique properties of cholesteric liquid crystals is the strong selective reflection of circularly polarized light with the same handedness as the helix, whereas the transmission of oppositely polarized light is not affected significantly.[4] For light propagating parallel to the helical axis the reflection range of the wavelength Λ (in vacuo) is given by $n_o|p| \leq \Lambda \leq n_e|p|$, where n_e and n_o are the extraordinary and ordinary refractive indices of the underlying nematic structure, respectively, and p is the helical pitch (with the sign of p indicating the handedness of the helix).

In cholesteric elastomers, a deformation of the helical structure by mechanical stress is accompanied directly by changes in the transmission spectra. Biaxial stress applied perpendicular to the helical axis leads to a contraction of the pitch, which is affine to the change of the sample dimension along the helical axis.[5,6] Apart from this, no further distortion of the regular helical structure was found.

For uniaxial mechanical stress the situation is more complicated. It has been predicted theoretically[7−9] that uniaxial stress applied perpendicular to the helical axis should lead to a distortion of the regular helix in addition to the affine pitch contraction. Above a critical strain the director is expected to describe no longer complete rotations but to oscillate around a preferred direction. Band structure calculations[10] resulted in regions of reflection partially expected as independent of the polarization of incident light. The theory was partially proven by Cicuta et al. by means of wide-angle X-ray scattering[11] and polarized light transmission[11,12] of cholesteric elastomer films prepared by using the anisotropic deswelling method.[13] However, up to now all these experiments were based on cholesteric elastomers showing a prolate main chain conformation.

The coupling of the mesogenic groups to the main chain by flexible spacer groups contributes to the anisotropic interaction of the mesogens with the main chain segment. For an odd number of atoms in the spacer chain one usually obtains prolate main chain conformations, whereas for an even number (and not too long spacer chains) a tendency for oblate conformations is observed in nematic elastomers.[14−16] This is reasonable because molecular models with a spacer chain in all-trans conformation and an even number of atoms show an orientation of the mesogenic group perpendicular to the main chain.

In this paper we present the preparation of a series of cholesteric elastomers with a polysiloxane backbone, where the molar fraction of two side groups with odd and even numbers of atoms along the short spacer chain was varied systematically. The resulting elastomers show a corresponding variation of the main chain conformation anisotropy from prolate to oblate. In contrast to the anisotropic deswelling method developed earlier,[13] we followed a technique using surface interactions to prepare free-standing cholesteric elastomer films.[6,17] These films show substantially improved optical properties in comparison with the samples obtained by the anisotropic deswelling

[†] CNRS.
[‡] Institut für Makromolekulare Chemie, Albert-Ludwigs-Universität.
[§] Physikalisches Institut, Albert-Ludwigs-Universität.
* Corresponding authors. E-mail: Heino.Finkelmann@makro.uni-freiburg.de, stille@uni-freiburg.de.

10.1021/ma061065a CCC: $33.50
Published on Web 10/19/2006

Table 1. Composition and Transition Temperatures of the Un-Cross-Linked Polymers[a]

x_{odd}	x_2	x_3	T_g/°C	T_{ci}/°C
0.0	0.810	0	26	92.2
0.1	0.729	0.081	22	92.2
0.2	0.648	0.162	21	88.9
0.3	0.567	0.243	20	87.9
0.4	0.486	0.324	20	86.8
0.5	0.405	0.405	23	91.8
0.6	0.324	0.486	20	92.2
0.7	0.243	0.567	19	92.2
0.8	0.162	0.648	18	95.5
0.9	0.081	0.729	17	95.2
1.0	0	0.810	16	97.8

[a] Relative molar content x_2 and x_3 of the side groups **2** and **3** with even and odd spacers, respectively, relative amount of odd spacer compound $x_{odd} = x_3/(x_2 + x_3)$, glass temperature T_g, and cholesteric−isotropic transition temperature T_{ci}. For all polymers: $x_4 = 0.02$ (photo-cross-linking compound **4**), $x_5 = 0.17$ (chiral side group **5**).

method.[11−13] This is also indicated by much lower threshold intensities in lasing experiments.[6] However, the surface interaction employed in the new method leads to a limitation of the film thickness. The transmission for polarized light under uniaxial mechanical stress applied perpendicular to the helical axis is studied and compared with the transmission calculated for the distorted helix structure predicted by theory.

Experimental Section

Materials. Cholesteric elastomer films of 20 μm thickness were synthesized according to a procedure which has been described in detail elsewhere.[17] A photo-cross-linkable polymer was synthesized via Pt-catalyzed hydrosilylation of poly[oxy(methylsilylene)] (DP ≈ 105). 60.1 mg (1 mmol of Si−H groups) of **1** and the appropriate amounts (see Table 1) of compounds **2**−**5** were dissolved in 1.5 mL of toluene. To the resulting solution, 10 μL of a 1 wt % solution of the Pt catalyst SLM86005 (Wacker Chemie, Burghausen) in dichloromethane was added. This solution was stirred at 60 °C in darkness. The addition of 10 μL of the catalyst solution was repeated after 5 h and after a further 14 h. The progress of the reaction was monitored by IR spectroscopy ($\nu_{Si-H} = 2160$ cm^{-1}). The resulting polymer was purified via reprecipitation (five times) from methanol. Dry-freezing yielded the photo-cross-linkable polymer (yield ≈ 80%).

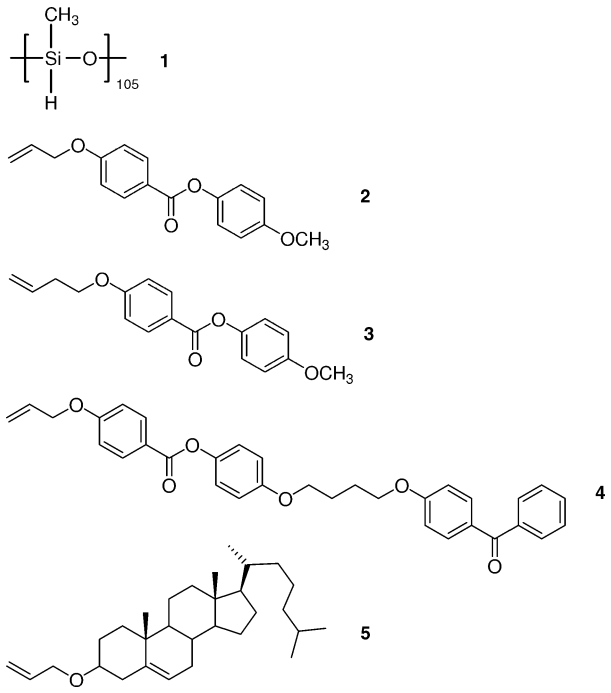

The cholesteric elastomers were prepared between two glass substrates covered with a water-soluble sacrificial layer of PEOX (poly(2-ethyl-2-oxazoline)). To obtain elastomers with a well-defined thickness, spacer foil strips of 20 μm thickness were used to adjust the distance between the two glass plates. The samples were then annealed within the liquid crystalline state for 2 days to achieve a Grandjean texture. The annealing temperatures were 8 K below the cholesteric−isotropic transition temperatures T_{ci} of the polymers. Because of interface interactions, well-ordered Grandjean textures were obtained. A defined surface alignment of the director was not ensured because it was not possible to rub the sacrificial layers in a preferred direction without destroying them. The orientation process of the liquid crystalline polymers was monitored by using visible light transmission spectroscopy and polarized optical microscopy. The oriented films were cross-linked when no improvement of the selective reflection band was achieved by further annealing. The cross-linking process is based on the radical reaction of the benzophenone derivative[18] **4** which is attached to the polymer backbone. To perform the cross-linking, the sample was irradiated by UV light from a "Philips E400" lamp for 15 min twice on each side. After the cross-linking process was completed, the resulting elastomer film was removed from the glass substrate by dissolving the sacrificial layers in water. In this way, 11 cholesteric elastomers with systematically varied content of compounds **2** and **3** as shown in Table 1 were prepared.

Transmission Electron Microscopy. The samples were embedded in epoxy resin and heated to 40 °C. Because of the soft nature of samples, the resulting material was then frozen at −90 °C and cut by ultramicrotomy (Reichert Ultracut equipped with a diamond knife) along a direction perpendicular to the film surfaces. The thickness of the cross sections was about 120 nm. The TEM investigations were carried out with a CM30 Philips microscope fitted with a 1024 × 1024 Gatan CCD camera.

Transmission Measurements. A well-collimated white light source with a beam diameter of about 1.5 mm in the sample plane was used for the transmission measurements. In the case of transmission of linearly polarized light the beam passed a polarizer prism oriented parallel and perpendicular to the direction of the sample strain, respectively. In the case of transmission of circularly polarized light, the linearly polarized beam additionally passed a "super-achromatic" quarter-wave retarder (B. Halle Nachfl. GmbH, Berlin), oriented with its fast axis at ±45° with respect to the plane of polarization. The sample film, mounted to allow an adjustable strain, was then passed by the polarized light at normal incidence. The transmitted light was guided by fiber optics to a spectrometer (Ocean Optics S2000) with a spectral resolution of 1.5 nm. All spectra were recorded at room temperature.

Theoretical Basis

The theory of Warner and Terentjev on liquid crystalline elastomers[9] does not treat the details of the anisotropic interaction between mesogenic groups and main chain (and hence cannot explain the odd−even effect of the spacer chains), but its result is considered as a random walk of the main chain segments with an anisotropic step length distribution. This is described by a step length tensor $\boldsymbol{l}$ with the components $l_{ij} = l_\perp[\delta_{ij} + (r - 1)n_i n_j]$. Here the anisotropy enters as the ratio $r = l_\parallel/l_\perp$ of the average step lengths $l_\parallel$ and $l_\perp$ parallel and perpendicular to the director **n**, respectively. The free energy density of a deformed nematic elastomer is calculated from the classical rubber shear modulus G, the step length tensor $\boldsymbol{l}_0$ of the undeformed state, the inverse step length tensor $\boldsymbol{l}^{-1}$ of the deformed state, and the deformation tensor $\boldsymbol{\lambda}$ as $f = {}^1/_2 G\,\mathrm{Tr}(\boldsymbol{l}_0\boldsymbol{\lambda}^T\boldsymbol{l}^{-1}\boldsymbol{\lambda})$.

This theory was also applied to cholesteric elastomers.[7,8] For uniaxial stress applied perpendicular to the helical axis, $\boldsymbol{\lambda}$ is assumed to be diagonal with the nonzero components λ_{xx}, λ_{yy}, and λ_{zz}, using a frame with the stress parallel to x and the helical axis parallel to z. Rubber volume is conserved in good

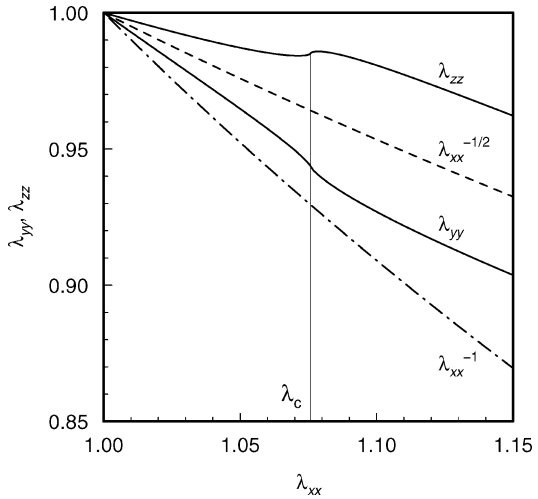

Figure 1. Deformations λ_{yy} and λ_{zz} of elastomer films, calculated numerically according to theory[7,8] in dependence of the deformation λ_{xx} for conformation anisotropies $r = 1.3$ or $r = 1/1.3$ (see text). Included are the power laws $\lambda_{xx}^{-1/2}$ for an isotropic contraction and λ_{xx}^{-1} for a contraction along only one dimension. The critical deformation $\lambda_c = 1 + \epsilon_c$ is indicated by the vertical line.

approximation, leading to the condition $\lambda_{xx}\lambda_{yy}\lambda_{zz} = 1$. The Frank elasticity contribution to the free energy is neglected. For the regular helix in the undeformed state the angle $\Phi_0 = 2\pi z/p_0$ between director and x axis is linearly depending on z. Here p_0 denotes the helical pitch. In the deformed state the corresponding angle Φ no longer depends linearly on z. With the director fields for the two states now the step length and inverse step length tensors are obtained, and the free energy density can be calculated and, for equilibrium, minimized with respect to Φ, resulting in

$$\tan(2\Phi) = \frac{2(r-1)\lambda_{xx}\lambda_{yy}\sin(2\Phi_0)}{(r-1)(\lambda_{xx}^2 + \lambda_{yy}^2)\cos(2\Phi_0) + (r+1)(\lambda_{xx}^2 - \lambda_{yy}^2)} \quad (1)$$

As the free energy density is a periodic function of Φ_0, the macroscopic free energy has to be calculated by integration over z. Then, for a given strain $\epsilon_{xx} = \lambda_{xx} - 1$ along the applied stress, the free energy is minimized numerically with respect to the deformations λ_{yy} and λ_{zz}, taking into account the volume conservation.

The calculated deformations $\lambda_{yy}(\lambda_{xx})$ and $\lambda_{zz}(\lambda_{xx})$ are shown in Figure 1. Originally the results were discussed for prolate conformations only.[7,8] However, the same considerations should apply also for oblate conformations. It turns out (see Figure 1) that one obtains the same deformations for a given value of the anisotropy ratio r (here $r = 1.3$) and its inverse (here $r = 1/1.3$), i.e., if the step lengths $l_{\parallel}$ and $l_{\perp}$ of a prolate conformation are interchanged to result in a corresponding oblate conformation. Also, the macroscopic free energy is the same for a given value of r and its inverse. λ_{yy} is lower than $\lambda_{xx}^{-1/2}$, which would be the contraction of an isotropic rubber. Correspondingly, the contraction λ_{zz} is larger, indicating a stiffening for deformations along the helical axis. The helix pitch is contracted by the same factor λ_{zz} as the complete layer.

In addition to this affine contraction the calculation results in helix distortions given by the director orientation angle $\Phi(z)$, different for prolate and oblate conformation anisotropies. Calculations of $\Phi(z/p)$ (with p denoting the pitch of the distorted helix), using $\lambda_{yy}(\lambda_{xx})$ and eq 1, are shown in Figure 2. The straight lines for $\epsilon_{xx} = 0$ correspond to the linear dependence

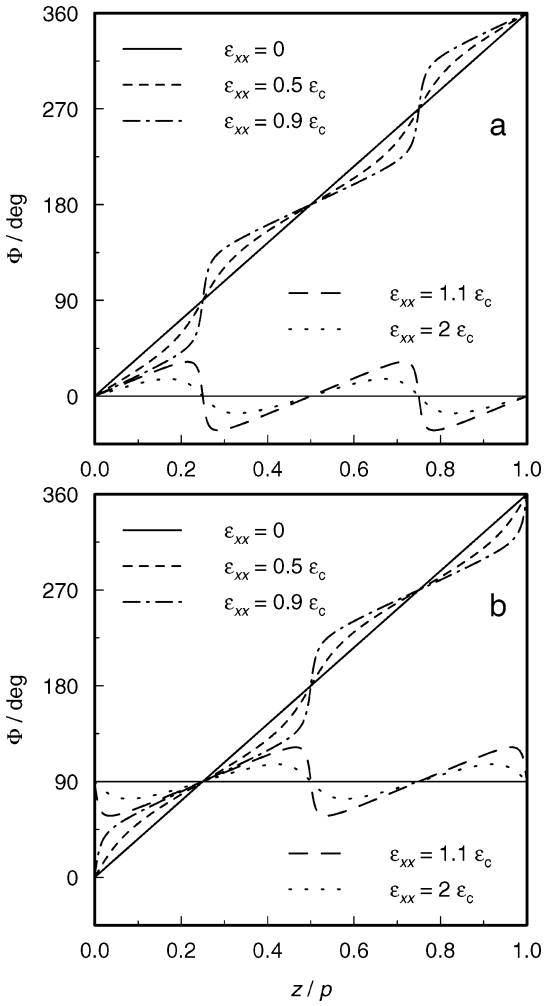

Figure 2. Director orientation angle $\Phi(z/p)$ of elastomer films, calculated numerically according to theory[7,8] for different strains ϵ_{xx} in units of the critical strain $\epsilon_c = 0.0758$ (a) for a prolate conformation anisotropy $r = 1.3$ and (b) for an oblate conformation anisotropy $r = 1/1.3$ (see text).

for an undistorted helix. For small strains one observes deviations whereby the director tends to orient parallel to the stress direction x in the case of a prolate conformation and perpendicular to stress in the case of an oblate one. Above a critical strain $\epsilon_c = \lambda_c - 1$ depending on r ($\epsilon_c = 0.0758$ for $r = 1.3$ and $r = 1/1.3$), the rotation of the director is not longer complete: Φ oscillates around 0 in the case of prolate and around 90° in the case of oblate conformations. It can be shown that $\Phi(r^{-1},\Phi_0) = \Phi(r,\Phi_0 - \pi/2) + \pi/2$, i.e., that for the symmetry of the distortion the roles of x and y axes interchange when going from a prolate conformation to a corresponding oblate one with an inverted value of r. For strains close to ϵ_c there are narrow regions of high twist. Slightly before the critical deformation λ_c the contraction factors λ_{yy} and λ_{zz} start to deviate from their initial behavior (see Figure 1). λ_{zz} passes a maximum. Around λ_c, the elastomers are expected to show a coexistence of regions with two differently distorted helices of finite twist.[9]

The distortions of the helical structure should lead to changes in the transmission spectra as shown by band structure calculations,[10] which predict regions of reflection, partially independent of the polarization of incident light.

Results

Our aim is to obtain a deeper understanding of the strain-induced structural changes in cholesteric elastomers by analyzing

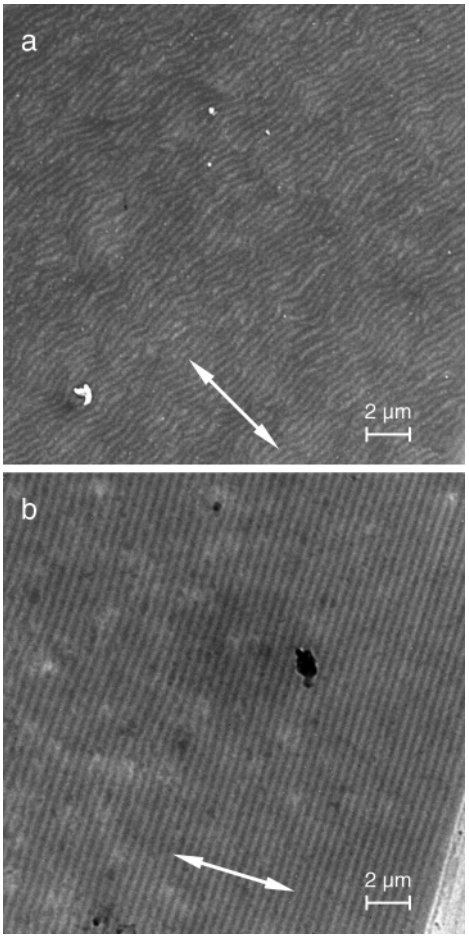

Figure 3. TEM micrographs of cholesteric elastomer films obtained by the anisotropic deswelling method (a) and by photo-cross-linking a well-aligned cholesteric polymer film (b). Cross sections along a direction perpendicular to the film surfaces are shown. Lines of equal brightness correspond to quasi-nematic planes with uniform orientation of the director in relation to the plane of observation. The average orientation of the cholesteric helix axes is indicated by double arrows.

the optical properties. For a detailed study of the changes in the transmission spectra, well-ordered cholesteric networks with good optical quality are indispensable. So far, uniaxial deformation experiments have only been performed using samples obtained by the anisotropic deswelling method. TEM investigations of such elastomers reveal a high density of microscopic defects and undulations (Figure 3a). The disordered structure gives rise to poor optical quality and probably to an inhomogeneous response to mechanical fields. In contrast, elastomers obtained by the photo-cross-linking method show almost perfect periodicity of the liquid-crystalline order (Figure 3b), resulting in substantially improved optical quality.[6] Using this improved preparation technique, we synthesized a series of samples with different conformation anisotropies and studied their mechanical and optical properties.

Temperature Dependence of Sample Dimensions. Figure 4 shows the temperature dependence of the reduced sample lengths $L_{red} = L_x/L_{x,iso}$ for several elastomers. The sample dimension L_x was measured perpendicular to the helical axis at zero stress. No clear discontinuity is observed at the phase transition. For elastomers prepared in the cholesteric state theory expects that, because of internal constraints, the main chain conformation will not get completely isotropic at high temperatures above the phase transition.[9] The remaining conformation anisotropy in return should induce a nonvanishing orientational order of the mesogenic groups, corresponding to a susceptibility

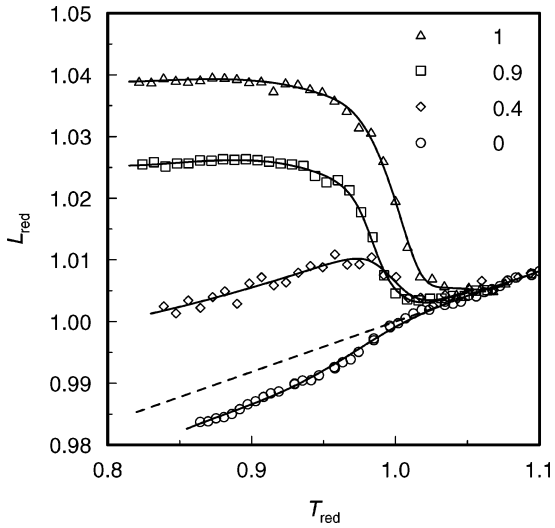

Figure 4. Dependence of the reduced sample lengths L_{red} (measured perpendicular to the helical axis) on the reduced temperature $T_{red} = T/T_{ci}$ for several elastomers with different relative molar fractions x_{odd} of the nematic side group compound **3**. The dashed line indicates the expected dependence for an isotropic conformation obtained by extrapolation from a fit to the data of the isotropic phase.

in the isotropic state, decreasing with increasing temperature. In fact, it was found by temperature-dependent measurements of the birefringence of cholesteric elastomers and the corresponding un-cross-linked polymers that a clear discontinuity did vanish after cross-linking.[19]

In the case of the sample with the smallest change at the phase transition ($x_{odd} = 0$), for $L_{x,iso}$ a value was taken as measured in the isotropic phase close to the phase transition temperature T_{ci}. For the other elastomers, $L_{x,iso}$ was adjusted in a way that the values of L_{red} match at high temperatures. The elastomer without any content of the even spacer compound ($x_{odd} = 1$) shows a dependence as expected for a locally prolate conformation: In the cholesteric phase only the smaller component $l_\perp$ contributes to the direction parallel to the helical axis, whereas the rotating nematic director leads to an elongation measured perpendicular to the helical axis, caused by a larger average of the components $l_\parallel$ and $l_\perp$. In the isotropic phase this elongation vanishes because of $l_\parallel = l_\perp$. With reduced content of the odd spacer compound the conformation anisotropy decreases, and for $x_{odd} = 0$ we observe $L_{red} < 1$ in the cholesteric phase, indicating an oblate conformation. Obviously, for all samples an ordinary thermal expansion is superposed to the (quite small) anisotropy effect on the sample length. The dashed straight line in Figure 4 was obtained by a fit to the values of the isotropic phase. The linear thermal expansion coefficient α_l can be calculated from the slope of that line:

$$\alpha_l = \frac{1}{L}\frac{dL}{dT} = \frac{1}{L_{red}T_{ci}}\frac{dL_{red}}{dT_{red}} \approx \frac{1}{T_{ci}}\frac{dL_{red}}{dT_{red}}$$

$$\approx \frac{0.0816}{365\ \mathrm{K}} = 2.24 \times 10^{-4}\ \mathrm{K}^{-1}$$

This value corresponds very well with those found for commercial silicon rubbers. The fitted line was extrapolated to lower temperatures to obtain a correction factor for compensating the thermal expansion effect in L_{red}. The values $L_{red,corr}$ at room temperature, corrected in this way, are shown in Table 2.

Cholesteric and nematic liquid crystals are known to show a small discontinuous volume increase at the transition to the isotropic phase. This was also found by PVT measurements for

Table 2. Calculated Conformation Anisotropies and Critical Strains[a]

x_{odd}	$L_{red,corr}$	r	ϵ_c
0.0	0.995	0.94	0.0175
0.4	1.016	1.20	0.052
0.9	1.041	1.55	0.129
1.0	1.055	1.76	0.169

[a] Relative amount of odd spacer compound x_{odd}, corrected reduced length $L_{red,corr}$, conformation anisotropy r, and critical strain ϵ_c at room temperature, calculated according to theory[7,8] for the elastomers shown in Figure 4.

nematic side chain polymers.[20] Typical values of the relative volume change are $\Delta V_{ni}/V \approx 0.3\%$, both for low molar mass and polymeric compounds. Assuming similar values for nematic side chain elastomers as well as isotropic changes of the sample dimensions, this would lead to a relative length change $\Delta L_{ni}/L \approx {}^1/_3 \Delta V_{ni}/V \approx 0.1\%$. With the exception of the sample with $x_{odd} = 0$, the effect on $L_{red,corr}$ then should be negligible (see Table 2). For symmetry reasons, however, the volume change in general should result in an anisotropic shape change.

The values of $L_{red,corr}$ were then used to calculate the conformation anisotropy r from the theoretically predicted length change of cholesteric elastomers,[9] neglecting possible consequences of the volume change at the phase transition. The change of sample dimensions is described corresponding to the transition of a unit cube in the cholesteric state to a quadratic prism of unit volume $\lambda_{xx}\lambda_{yy}\lambda_{zz} = 1$. Assuming an anisotropy r in the cholesteric state at room temperature (when the photo-cross-linking was performed), the height λ_{zz} of the prism (dimension parallel to the helix axis) results as

$$\lambda_{zz} = \left(\frac{r+1}{2}\right)^{1/3} \tag{2}$$

Our quantity $L_{red,corr}$ corresponds to the length in x direction related to the value in the isotropic state and is therefore given as

$$L_{red,corr} = {\lambda_{xx}}^{-1} = {\lambda_{yy}}^{-1} = {\lambda_{zz}}^{1/2} = \left(\frac{r+1}{2}\right)^{1/6} \tag{3}$$

which yields an estimate

$$r = 2L_{red,corr}^{6} - 1 \tag{4}$$

for the conformation anisotropy. Table 2 shows the results at room temperature, where the photo-cross-linking was performed.

Transmission Spectra. In Figure 5 the transmission τ of circularly polarized light in the wavelength range 400 nm $\leq \Lambda \leq$ 900 nm is shown for three elastomers at different strains by stress applied perpendicular to the helical axis. The upper row contains the spectra for zero strain. Transmission gaps due to selective reflection are found for left circularly polarized light, corresponding to left-handed cholesteric helices. Because of scattering, a decreased transmission is obtained at short wavelengths. Interference fringes are only observed far from the band edges which are not as sharp as in calculated spectra of perfect cholesteric layers. There might still be some distribution of pitches or helical axes in the samples. However, the optical quality has improved compared to that of elastomers obtained in the past by the anisotropic deswelling method.[13]

The center wavelength of the selective reflection band of a cholesteric layer at normal incidence is given by[4]

$$\Lambda_R = |p_0|\sqrt{\frac{1}{2}({n_e}^2 + {n_o}^2)} \tag{5}$$

It is shown in Figure 6 for all unstrained elastomer samples. A red shift of Λ_R with increasing values of x_{odd} is observed. The refractive indices n_e and n_o do not vary much. Therefore, this indicates that for increasing average spacer lengths (high values of x_{odd}) the rotation of the mesogenic units around their long axes is less restricted, resulting in lower local biaxiality and causing lower twist and higher values of the helical pitch $|p_0|$.

Within a column of spectra in Figure 5, an increasing strain results in a blue shift of the center wavelength. For biaxial stress a pitch decrease affine to the shrinkage of the samples along the helical axis was observed;[6] that means the number of director turns is conserved as the sample changes its thickness. We assume that the number of periods is conserved for uniaxial stress, too, in accordance with the theoretical predictions. The reduced center wavelength $\Lambda_{red}(\lambda_{xx}) = \Lambda_R(\lambda_{xx})/\Lambda_R(\lambda_{xx} = 1)$

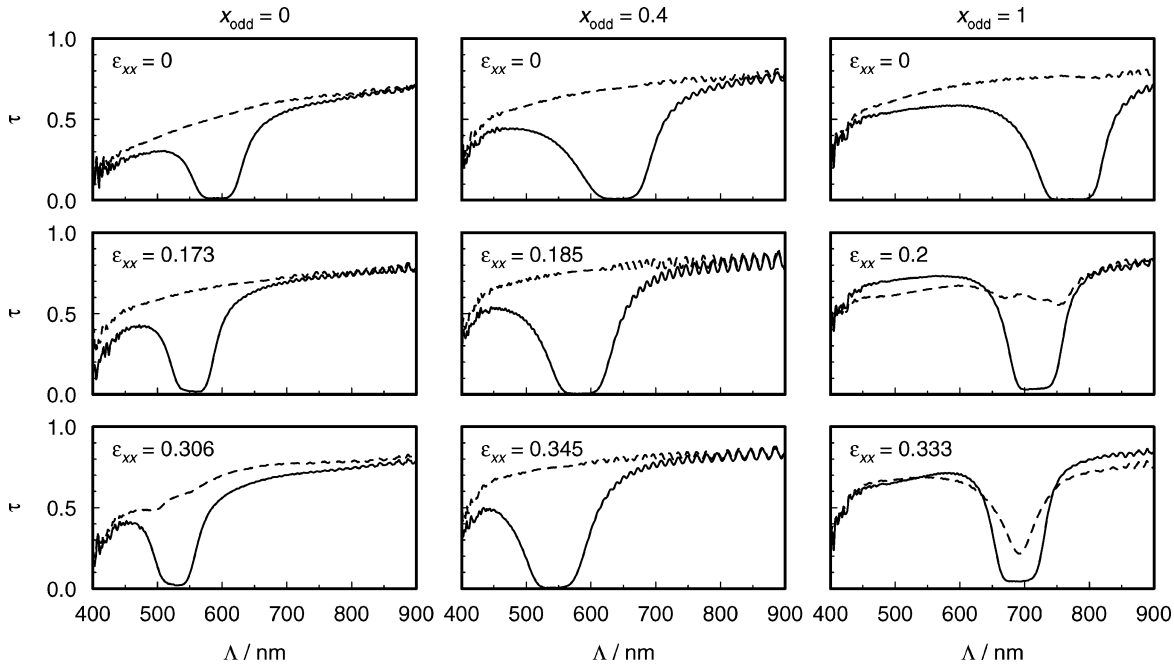

Figure 5. Transmission spectra of three elastomers with different relative molar fractions x_{odd} for left (solid curves) and right circularly polarized light (dashed curves) at room temperature for different uniaxial strains ϵ_{xx} perpendicular to the helical axis.

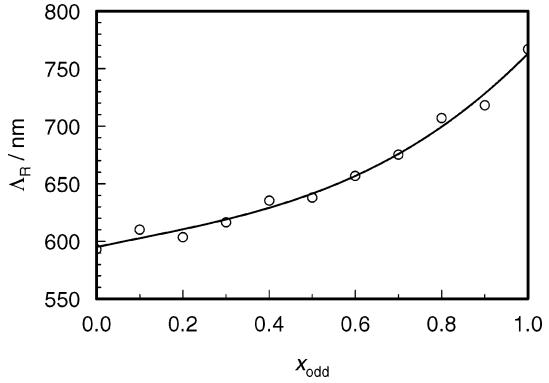

Figure 6. Dependence of the center wavelength Λ_R of the unstrained elastomers on the relative molar fraction x_{odd}.

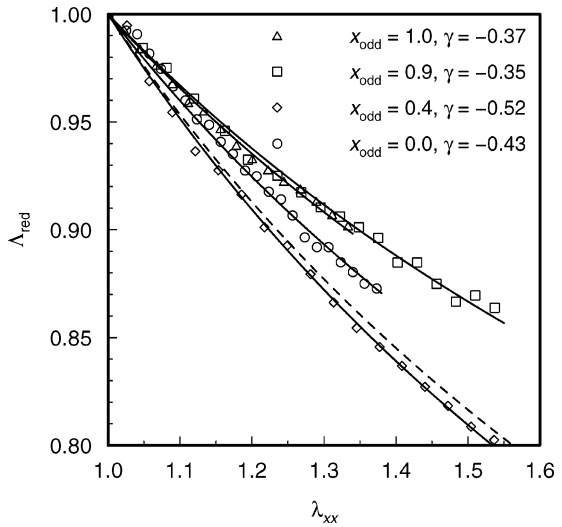

Figure 7. Dependence of the reduced center wavelength Λ_{red} of several elastomers with different relative molar fractions x_{odd} on the deformation $\lambda_{xx} = 1 + \epsilon_{xx}$. Solid lines: fits to the power law λ_{xx}^{γ}. Dashed line: expected power law for isotropic contraction ($\gamma = -1/2$).

should then be equal to the sample contraction along the helical axis $\lambda_{zz}(\lambda_{xx})$. For an incompressible rubber with isotropic main chain conformation it should follow the power law $\Lambda_{red}(\lambda_{xx}) = \lambda_{xx}^{\gamma}$ with an exponent $\gamma = -1/2$. The experiments can be well described by empirical fits to the power law (see Figure 7). For the sample with $x_{odd} = 0.4$ an exponent close to $-1/2$ was found, as expected for a vanishing conformational anisotropy. This is in contrast to the temperature dependence of the sample length, which seems to indicate a significant prolate anisotropy. The other samples (prolate and oblate) show larger exponents according to a stiffening for dimension changes along the helical axis.

Indeed, a stiffening was predicted by the theory in the case of anisotropic chain conformations. Using the conformation anisotropies r obtained from the measurements of the reduced sample lengths (see Table 2), the contractions along the helical axis $\lambda_{zz}(\lambda_{xx})$ are calculated according to the theory and compared with the experimental values of Λ_{red} in Figure 8. Only for the sample with the weakest anisotropy ($x_{odd} = 0.0$, $r = 0.94$) the experimental values are not far from the theoretical curves. They do not match the details near the critical strain and the expected slopes for the two samples with the highest values of r. For the sample with $x_{odd} = 0.4$ the corresponding value of $r = 1.20$ indicates a significant prolate anisotropy, again in contrast to the observed values of Λ_{red} according to nearly isotropic contraction.

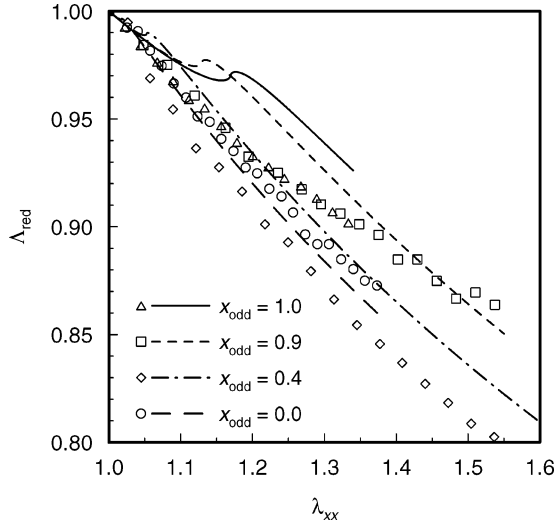

Figure 8. Comparison of the reduced center wavelength Λ_{red} (symbols) of several elastomers with different relative molar fractions x_{odd} with the contractions λ_{zz} (lines) calculated numerically according to the theory,[7,8] using the corresponding conformation anisotropies r at room temperature obtained from the sample length measurements (see Table 2).

Looking again on the transmission spectra for circularly polarized light in Figure 5, one observes a pronounced transmission drop also for right circularly polarized light in the case of the sample with the strongest prolate anisotropy ($x_{odd} = 1$) at the highest strain value ($\epsilon_{xx} = 0.333$). This corresponds to the theoretical prediction of a complete band gap in the sense of reflection independent of the polarization of the incident light,[10] which has been also demonstrated experimentally.[12]

Figure 9 shows the transmission τ for light linearly polarized parallel and perpendicular to the direction of the applied mechanical stress. For the unstrained elastomers in the upper row nearly equal transmissions are observed for both polarizations, as to be expected. In the case of the strongest prolate sample with $x_{odd} = 1.0$ for light polarized parallel to stress with increasing strain, a transmission decrease is observed close to the long wavelength band edge and for perpendicular polarization a decrease close to the short wavelength edge. In the case of the weakly oblate sample with $x_{odd} = 0$ the opposite behavior is observed: a decrease at short wavelengths for parallel and at long wavelengths for perpendicular polarization. This corresponds to the interchanged roles of the x and y axes in the theoretically calculated distortion $\Phi(z/p)$ for prolate and oblate conformations. In correspondence to the observation for circular polarization, in the case of the sample with the strongest prolate anisotropy at the highest strain value, strong transmission drops nearly independent of polarization are observed close to the center wavelength.

For the sample with $x_{odd} = 0.4$ a weak, but significant, prolate anisotropy $r = 1.20$ was calculated. However, we got nearly equal transmissions for both polarizations even for nonvanishing strain, as to be expected for an isotropic conformation. Assuming a vanishing conformation anisotropy ($r \approx 1$) in the cholesteric state, the volume change at the phase transition could cause the observed change of the sample length, if it corresponds to an anisotropic shape change. To result in a typical volume reduction $V/V_{iso} \approx 0.997$ at the transition from the isotropic to the cholesteric state, an expansion of $L_x/L_{x,iso} = L_y/L_{y,iso} \approx 1.016$ (see Table 2) perpendicular to the helix axis then would have to be overcompensated by a shrinkage $L_z/L_{iso} = V/V_{iso}/(L_x/L_{x,iso})^2 \approx 0.966$ along the helix axis. Assuming similar anisotropic shape change contributions originating from the volume change also

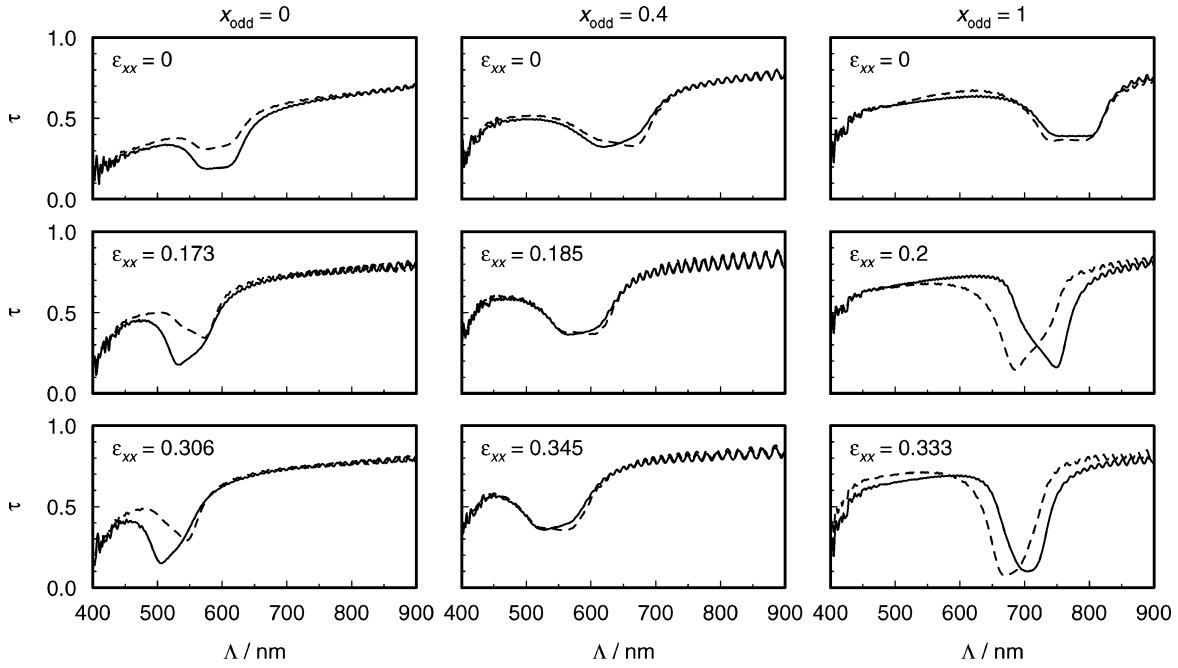

Figure 9. Transmission spectra of three elastomers with different relative molar fractions x_{odd} for light linearly polarized parallel (solid curves) and perpendicular (dashed curves) to the direction of stress at room temperature for different uniaxial strains ϵ_{xx}.

for the other samples, this would lead to smaller values of r than that given in Table 2. However, the consequences would be less drastic for the samples with a stronger conformation anisotropy, and the corresponding discrepancies observed in Figure 8 would remain.

Calculated Spectra. When calculating the director orientation angle Φ using eq 1 it turns out that for moderate prolate and oblate conformation anisotropies $1 < r < 2$ and $^1/_2 < r < 1$, respectively, the corresponding functions $\Phi(z/p)$ are nearly independent of r for equal strains in units of the critical strains, i.e. for equal reduced strains $\epsilon_{red} = \epsilon_{xx}/\epsilon_c$. For comparison with the experiments, transmission spectra of distorted cholesteric elastomer layers were calculated by the fast version[21] of the Berreman 4 × 4 matrix algorithm,[22] using the dependencies $\Phi(z/p)$ predicted by theory. Refractive index values $n_e = 1.6543$ and $n_o = 1.5226$ of the quasi-nematic layers as obtained from measurements with an Abbe refractometer[6] were used. The refractive index of the surrounding medium was set to $n = 1$. The cholesteric elastomer film was assumed to have 50 director turns of a left-handed helix along its normal. Taking into account the missing uniform surface alignment, the transmission was calculated for different orientations of the director in the surface plane and averaged. The results are shown in Figure 10 for a prolate conformation ($r = 1.3$). Since for the symmetry of the distortion of the helix for a corresponding oblate conformation ($r = 1/1.3$) x and y axes just interchange their role, the circularly polarized spectra are the same as for the prolate case, and the parallel and perpendicular linearly polarized spectra would have to be interchanged. We therefore show only the calculations for a prolate conformation anisotropy.

For a small reduced strain $\epsilon_{red} = 0.25$ the main effect is the asymmetry of the two linearly polarized spectra, similar to the experimental observations shown in Figure 9. For $\epsilon_{red} = 0.5$ a narrow central drop in transmission was observed. For $\epsilon_{red} = 0.9$ the central part is wider and its reflection is complete, independent of polarization. Sidebands, asymmetric in the case of linear polarization, are seen in all of the spectra. For $\epsilon_{red} = 2$ the sidebands have vanished (continuously with increasing strain, not shown); the remaining central part starts to get narrower again. For even larger strains (not shown) the central drop gets narrower and finally less pronounced as the undulations of the director field are more and more suppressed.

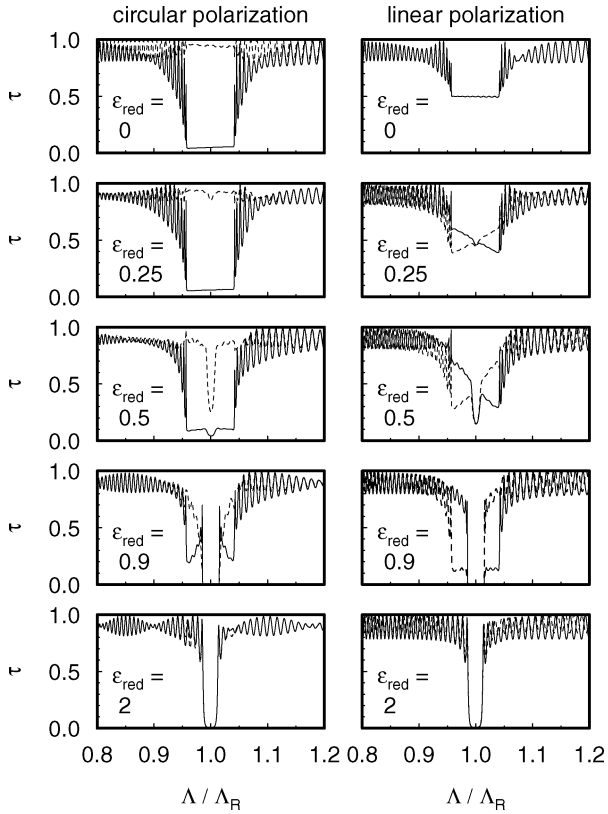

Figure 10. Transmission τ of cholesteric elastomer films in dependence of the reduced wavelength Λ/Λ_R, calculated numerically according to theory[7,8] for a prolate conformation anisotropy $r = 1.3$ at different reduced strains $\epsilon_{red} = \epsilon_{xx}/\epsilon_c$. Left: transmission of left (solid curves) and right (dashed curves) circularly polarized light. Right: transmission of light linearly polarized parallel (solid curves) and perpendicular (dashed curves) to the direction of stress; for an oblate conformation with $r = 1/1.3$ the two linearly polarized spectra would have to be interchanged for each reduced strain.

For comparison with the strains of the spectra shown in Figures 5 and 9, the theoretically expected critical strains ϵ_c of the samples, calculated numerically from the conformation anisotropies r, are given in Table 2. The values of ϵ_c are all significantly lower than the corresponding strains of the spectra for nonzero strain. This still should be the case when smaller values of r would have been used, taking into account an anisotropic shape change contribution originating from the volume change at the phase transition. Therefore, from theory one should expect spectra showing only the central part similar to that for $\epsilon_{red} = 2$ in Figure 10, independent of polarization. However, all experimental nonzero strain spectra are still strongly dependent on polarization, and a strong central drop in the right circularly polarized spectrum is observed only for the strongest prolate conformation at the highest strain (see Figure 5). In particular, the linearly polarized nonzero strain spectra of Figure 9, in comparison with Figure 10, suggest small reduced strains around $\epsilon_{red} \approx 0.25$.

The reason for this discrepancy is not clear. Maybe the domain structure due to the missing surface alignment plays a role. Possibly Frank elasticity cannot be neglected completely. This can be discussed regarding the nematic penetration depth[9]

$$\xi = \frac{1}{|r-1|}\sqrt{\frac{K_2}{G}} \tag{6}$$

where K_2 denotes the twist elastic constant. Assuming reasonable values $K_2 \approx 10^{-11}$ N (typical for low molar mass liquid crystals and non-cross-linked nematic side chain polymers[23]), $G \approx 10^6$ N m^{-2} and $|p_0| \approx 0.4 \times 10^{-6}$ m, this results in a ratio of $|p_0|/\xi \approx 100$ for $r = 1.8$, but only of ≈ 8 for the weakest calculated anisotropy $r = 0.94$, indicating a nonnegligible Frank elasticity contribution. Finally, instead of ideal soft elasticity, which results from the theory for ideal nematic elastomers, semisoftness[9] might have to be considered in a theoretical description of our real elastomers. Soft elasticity means that for an "ideal" single domain nematic elastomer a rotation of the nematic director accompanied by a corresponding shape change should be possible without cost of energy.[24,25] The term semisoft elasticity is used to describe nonvanishing torques, experimentally observed for such rotations in real nematic elastomers. In the case of cholesteric elastomers a pure soft elastic deformation is not possible; however, the stiffening for contractions along the helical axis resulting in $\lambda_{zz}(\lambda_{xx})$ is considered as a compromise between hard ($\lambda_{zz} = \lambda_{xx}^{-1/2}$) and soft response ($\lambda_{zz}$ = constant).[9]

It should be mentioned that in the experiments of Cicuta et al.[12] on cholesteric elastomers obtained by the anisotropic deswelling method[13] a band of complete reflection nearly independent of polarization at $\epsilon_{xx} \approx 0.1$ was found as to be expected from theory for $\epsilon_{xx} > \epsilon_c$, but values of the conformation anisotropy and the critical strain were not given.

Conclusions

In this paper we presented the preparation and optical characterization of a series of cholesteric elastomers with conformations varying from prolate to oblate. The conformation anisotropy was calculated from temperature-dependent measurements of the sample dimensions. The effect of uniaxial stress perpendicular to the helical axis on the helix structure was studied by the transmission of polarized light. The stiffening for deformations along the helical axis, predicted by theory, was confirmed qualitatively. However, the strain dependence of the observed contraction along the helical axis showed deviations from theory. In particular, it did not show the details around the predicted critical strain, above which the director should no longer rotate completely. The transmission spectra indicate that the distortion of the helix is much weaker than predicted theoretically. The reason for this discrepancy is not yet understood.

For one of the samples the transmission spectra indicated a vanishing conformation anisotropy, in contrast to the observed length change at the phase transition. This can be explained in accordance with an isotropic conformation in the cholesteric state, if the decrease in volume at the transition from the isotropic to the cholesteric state is assumed to cause an anisotropic shape change. Unfortunately, the consequence of the volume change at the phase transition on the shape of liquid crystalline elastomers has not been studied so far. Taking into account such a shape change contribution also for the other samples, one would obtain slightly smaller values of the step length ratio r.

Additional studies should be carried out in the future, if the cholesteric elastomer films can be improved further by uniform surface alignment of the director, using appropriate materials for the sacrificial layers.

Acknowledgment. Thanks are due to the Deutsche Forschungsgemeinschaft (SFB 428) and the Fonds der Chemischen Industrie for financial support. W.S. thanks Prof. M. Warner for helpful discussions.

References and Notes

(1) Finkelmann, H.; Kock, H. J.; Rehage, G. *Makromol. Chem., Rapid Commun.* **1981**, *2*, 317−322.
(2) Kirste, R. G.; Ohm, H. G. *Makromol. Chem., Rapid Commun.* **1985**, *6*, 179−185.
(3) Moussa, F.; Cotton, J. P.; Hardouin, F.; Keller, P.; Lambert, M.; Pepy, G.; Mauzac, M.; Richard, H. *J. Phys. (Paris)* **1987**, *48*, 1079−1083.
(4) de Vries, H. *Acta Crystallogr.* **1951**, *4*, 219−226.
(5) Finkelmann, H.; Kim, S. T.; Muñoz, A. M.; Palffy-Muhoray, P.; Taheri, B. *Adv. Mater.* **2001**, *13*, 1069−1072.
(6) Schmidtke, J.; Kniesel, S.; Finkelmann, H. *Macromolecules* **2005**, *38*, 1357−1363.
(7) Warner, M.; Terentjev, E. M.; Meyer, R. B.; Mao, Y. *Phys. Rev. Lett.* **2000**, *85*, 2320−2323.
(8) Mao, Y.; Terentjev, E. M.; Warner, M. *Phys. Rev. E* **2001**, *64*, 041803.
(9) Warner, M.; Terentjev, E. M. *Liquid Crystal Elastomers*; Clarendon Press: Oxford, 2003.
(10) Bermel, P. A.; Warner, M. *Phys. Rev. E* **2002**, *65*, 056614.
(11) Cicuta, P.; Tajbakhsh, A. R.; Terentjev, E. M. *Phys. Rev. E* **2002**, *65*, 051704.
(12) Cicuta, P.; Tajbakhsh, A. R.; Terentjev, E. M. *Phys. Rev. E* **2004**, *70*, 011703.
(13) Kim, S. T.; Finkelmann, H. *Macromol. Rapid Commun.* **2001**, *22*, 429−433.
(14) Finkelmann, H.; Kock, H. J.; Gleim, W.; Rehage, G. *Makromol. Chem., Rapid Commun.* **1984**, *5*, 287−293.
(15) Guo, W.; Davis, F. J.; Mitchell, G. R. *Polymer* **1994**, *35*, 2952−2961.
(16) Greve, A.; Finkelmann, H. *Macromol. Chem. Phys.* **2001**, *202*, 2926−2946.
(17) Komp, A.; Rühe, J.; Finkelmann, H. *Macromol. Rapid Commun.* **2005**, *26*, 813−818.
(18) Prucker, O.; Naumann, C. A.; Rühe, J.; Knoll, W.; Frank, C. W. *J. Am. Chem. Soc.* **1999**, *121*, 8766−8770.
(19) Kniesel, S. Ph.D. Thesis, Albert-Ludwigs-Universiät, Freiburg, Germany, 2005.
(20) Frenzel, J.; Rehage, G. *Makromol. Chem., Rapid Commun.* **1980**, *1*, 129−134.
(21) Wöhler, H.; Haas, G.; Fritsch, M.; Mlynski, D. A. *J. Opt. Soc. Am. A* **1988**, *5*, 1554−1557.
(22) Berreman, D. W. *J. Opt. Soc. Am.* **1972**, *62*, 502−510.
(23) Schmidtke, J.; Stille, W.; Strobl, G. *Macromolecules* **2000**, *33*, 2922−2928.
(24) Warner, M.; Bladon, P.; Terentjev, E. M. *J. Phys. II* **1994**, *4*, 93−102.
(25) Olmsted, P. D. *J. Phys. II* **1994**, *4*, 2215−2230.

MA061065A